REDOX and anti-oxidant state within cattle oocytes following in vitro maturation with bone morphogenetic protein 15 and follicle stimulating hormone

Melanie L Sutton-McDowall [1,2,3,8], Malcolm Purdey [2,3]; Hannah M Brown [1], Andrew Abell [2,3]; David G Mottershead [1], Pablo D Cetica [4], Gabriel C Dalvit [4], Ewa M Goldys [2,5]; Robert B Gilchrist [1,7], David K Gardner [6] & Jeremy G Thompson [1,2,3]

[1] Robinson Research Institute, School of Paediatrics and Reproductive Health, The University of Adelaide, Medical School, Frome Road, Adelaide, South Australia, 5005, Australia

[2] Australian Research Council Centre of Excellence for Nanoscale BioPhotonics

[3] Institute for Photonics and Advanced Sensing, The University of Adelaide, North Terrace, Adelaide, South Australia, 5005, Australia

[4] Institute of Research and Technology on Animal Reproduction, School of Veterinary Sciences, University of Buenos Aires, Chorroarín 280, Buenos Aires C1427CWO, Argentina

[5] MQ BioFocus Research Centre, Macquarie University, North Ryde New South Wales 2109, Australia

[6] Department of Zoology, The University of Melbourne, Royal Parade, Parkville, Victoria 3010, Australia

[7] Current address: School of Women's & Children's Health, Discipline of Obstetrics & Gynaecology, University of New South Wales, Sydney 2052, Australia

[8] Corresponding author: melanie.mcdowall@adelaide.edu.au. Address: Medical School South, Frome Road, Adelaide, South Australia 5005 Australia. Telephone: +61 (8) 8313 1013. Facsimile: +61 (8) 8313 8177

FUNDING: This study was funded by National Health and Medical Research Council Australia Project (NHMRC, 1008137) and Development (1017484) grants and a collaborative research grant from Cook Medical (Eight Mile Plains, QLD Australia). JGT was funded by a NHMRC fellowship (627007). The Fluoview FV10i confocal microscope was purchased as part of the Sensing Technologies for Advanced Reproductive Research (STARR) facility, funded by the South Australia's Premier's Science and Research Fund. Furthermore, we acknowledge partial support of the Australian Research Council Centre of Excellence for Nanoscale BioPhotonics (CE140100003).

KEYWORDS: oocyte, bovine, BMP15, FSH, metabolism

ABRREVIATIONS: ASM = angular secondary moment; BMP15 = bone morphogenic protein 15; CC = cumulus cells; CDO = COC-derived denuded oocytes; COC = cumulus oocyte complex; FSH = follicle stimulating hormone; IDH = isocitrate dehydrogenase; IVM = in vitro oocyte maturation; G6PDH = glucose 6 phosphate dehydrogenase; GPX = glutathione peroxidase; GSH = reduced glutathione; GSR = glutathione reductase; GSS = glutathione synthetase; GSSG = oxidized glutathione; GSTA = glutathione S-transferase; ROS = reactive

oxygen species; MCB = monochlorobimane; OSF = oocyte secreted factors; PF1 = peroxyfluor 1.

ABSTRACT

Exogenous oocyte secreted factors such as bone morphogenetic protein 15 (BMP15), together with hormones traditionally used during *in vitro* oocyte maturation, increase the developmental competence of cumulus oocyte complexes (COCs). Separately, FSH and BMP15 induce different metabolic profiles within COCs, namely FSH increases glycolysis while BMP15 stimulates FAD and NAD(P)H auto-fluorescence within oocytes, without changing the REDOX ratio. Hence, the aim of this study was to investigate if BMP15-induced increased NAD(P)H was due to NADPH production. Cattle COCs were cultured with FSH and/or recombinant human BMP15 (BMP15). Following culture with BMP15, there was a significant decrease in glucose 6-phosphate dehydrogenase activity ($P<0.05$). Treatment with an inhibitor of isocitrate dehydrogenase (IDH) decreased NAD(P)H intensity 3-fold in BMP15 treated oocytes, suggesting BMP15 stimulates IDH and NADPH production via the TCA cycle. As NADPH is a reducing agent, reduced glutathione (GSH), H_2O_2 and mitochondrial activity were measured. FSH alone decreased GSH levels within the oocyte, with the combination of BMP15 and FSH recovering levels. Expression of genes encoding glutathione-reducing enzymes were also lower in oocytes cultured in the presence of FSH. However, BMP15 supplementation promoted mitochondrial localisation patterns consistent with enhanced developmental competence. Metabolomics revealed there was significant consumption of glutamine and production of alanine by COCs +FSH +BMP15 compared to the control ($P<0.05$). Hence, this study demonstrates that BMP15 supplementation differentially modulates reductive metabolism and mitochondrial localisation within the oocyte. In comparison, FSH-stimulation alone decreases the oocyte's ability to regulate cellular stress and therefore utilizes other mechanisms to improve developmental competence.

INTRODUCTION

During the final stages of oocyte development and immediately prior to ovulation, the oocyte and surrounding specialised somatic cells (cumulus cells) exhibit a symbiotic relationship (Albertini et al. 2001; Matzuk et al. 2002), and are referred to as the cumulus oocyte complex (COC). Bi-directional communication between the two cell populations is critical for oocyte developmental competence (the ability of the oocyte to undergo successful fertilisation and embryo development) and is facilitated by paracrine and gap junction communication (Larsen and Wert 1988; Buccione et al. 1990a; Albertini et al. 2001). Cumulus cells provide the oocyte with nutrients and factors essential for maturation (Sutton et al. 2003; Krisher 2013). In return, the oocyte secretes growth factors (oocyte secreted factors; OSF), that facilitates differentiation of cumulus cells from other ovarian cells (Li et al. 2000), mucification and proliferation (Buccione et al. 1990; Salustri et al. 1990a; Salustri et al. 1990b), increases steriodogenesis (Vanderhyden and Macdonald 1998) and prevents apoptosis (Hussein et al. 2005). Growth differentiation factor 9 (GDF9) and bone morphogenetic protein 15 (BMP15) are members of the transforming growth factor beta superfamily and have been identified as key OSF (Su et al. 2004). In particular, BMP15 is potent promoter of oocyte developmental competence in large, mono-ovular species such as cattle (Hussein et al. 2006; Crawford and McNatty 2012).

We have previously reported that recombinant human BMP15 and follicle stimulating hormone (FSH; a potent stimulator of COC metabolism and a common media additive during IVM) supplementation significantly increases bovine oocyte developmental competence (as indicated by increased on-time blastocyst yield; –FSH –BMP15 = 28.4 ± 7.4% vs. +FSH +BMP15 = 51.5 ± 5.4% total blastocysts/cleaved; $P < 0.05$), yet when added individually, they stimulate different metabolic activities within COCs, despite similar blastocyst yields (+FSH = 44.4 ± 3.9 vs. +BMP15 = 41 ± 2.9% total blastocysts/cleaved; $P > 0.05$) (Sutton-McDowall et

al. 2012). FSH-stimulates glucose metabolism via glycolysis and the hexosamine biosynthetic pathway in cumulus cells, indicated by increased lactate production and mucification leading to cumulus expansion; while BMP15 alone stimulates oxidative phosphorylation (as measured by FAD auto-fluorescence) and increased NAD(P)H levels within oocytes. Furthermore, the influence of FSH and BMP15 on oocyte metabolism was mediated via cumulus cells, as the oocyte itself exhibits low levels of glycolytic activity (Sutton-McDowall et al. 2012) and increases in intra-oocyte FAD and NAD(P)H levels were only detected in cumulus enclosed oocytes (Sutton-McDowall et al. 2012).

While FAD is the oxidised co-factor of $FADH_2$ within Complex II of the respiratory chain (mitochondria), NAD(P)H represents both NADH and NADPH (Mayevsky and Chance 1982; Skala and Ramanujam 2010), which are reducing agents and co-factors involved in numerous metabolic pathways. NADH is a co-factor for several metabolic enzymes, such as lactate dehydrogenase (cytoplasmic), and is a proton donor within Complex I of the respiratory chain within mitochondria, thus oxidised to NAD^+. NADPH is a co-factor for several enzymes, including 6-phosphogluconate dehydrogenase during glucose metabolism through the pentose phosphate pathway (cytoplasmic), and isocitrate dehydrogenase (IDH; TCA cycle within the mitochondria). Although the auto-fluorescence technique utilised in our previous study was unable to distinguish between NADH and NADPH (Sutton-McDowall et al. 2012), in somatic cells the majority of NAD(P)H auto-fluorescence represents NADH (Chance et al. 1979). Because BMP15 stimulates COCs to increase oxidative phosphorylation over glycolysis, an increased REDOX ratio (FAD:NAD(P)H) was predicted. However, this was not observed (Sutton-McDowall et al. 2012). Hence, BMP15 could also increase the yield of intra-oocyte NADPH.

While the oocyte itself has a low capacity for glucose uptake and metabolism (Sutton-McDowall et al. 2010), the pentose phosphate pathway is thought to be important for oocyte maturation by the provision of substrates for *de novo* nucleic acid synthesis and therefore is the primary source of oocyte NADPH (Downs et al. 1998). However, this has been challenged recently by the demonstration that IDH within the TCA cycle supplies the majority of NADPH within mouse oocytes (Dumollard et al. 2007b). Furthermore, only NADP-dependent IDH activity is detected in bovine cumulus cells and oocytes (Cetica et al. 2003).

Regardless of the source, NADPH plays an important role in preventing overt levels of reactive oxygen species (ROS) within the oocyte. Thiol compounds such as glutathione are innate antioxidants, by donating hydrogens to convert hydrogen peroxide (H_2O_2) to water. Oxidised glutathione (GSSG) is reduced (GSH) by glutathione reductase (GSR) and glutathione S-transferase (GSTA), which requires NADPH as a co-factor. GSH is important to cellular health and in regards to the oocyte, acquisition of higher levels of reduced glutathione during oocyte maturation is associated with improved developmental competence (Takahashi et al. 1993; de Matos et al. 1995; Sanchez et al. 2013).

The aim of this study was to investigate the differential metabolic profiles of cattle COCs exposed to FSH and BMP15. In particular, we investigated the source of the increased NAD(P)H levels within the oocyte, following stimulation by BMP15 alone and the consequences of elevated NAD(P)H levels in respect to intra-oocyte levels of reduced glutathione, mitochondrial activity/localisation and ROS levels.

RESULTS

Experiment 1: Intra-oocyte glucose 6-phosphate dehydrogenase (G6PDH) activity

To determine if increased NAD(P)H auto-fluorescence within the oocyte, following exposure to BMP15, were due to increased G6PDH (pentose phosphate pathway), COCs were cultured in the presence of brilliant cresyl blue (BCB; metabolised by G6PDH), with BCB^- oocytes indicating active enzymatic activity. The proportion of BCB^- oocytes after 23 h of culture did not vary between the control, +FSH and +FSH +BMP15 treatments (**Figure 1**). However, there was a main effect of BMP15 supplementation, with the proportion of BCB^- oocytes following culture in +BMP15 -FSH significantly lower than all the other groups (control = 90.8 $\pm$ 3.4% vs. +BMP15 = 62.4 ± 5.7%; $P < 0.05$). As BMP15 treatment decreased G6PDH activity within the oocyte, these results suggest that the pentose phosphate pathway is not the primary source of NADPH following BMP15 stimulation.

Experiment 2: Intra-oocyte isocitrate dehydrogenase (IDH) activity and NAD(P)H levels

To determine if the increased NAD(P)H levels within the oocyte following culture in the presence of BMP15 alone was due to increased IDH activity (TCA cycle), COCs were cultured in the presence or absence of BMP15, followed by oxalomalate, an inhibitor of IDH. A dose of 1 mM was used as the presence of 5 mM resulted in high levels of background fluorescence in the 405 nm excitation/420-520 nm emission spectrum (blue filter, **Supplementary Figure S1)**. Autofluorescence (NAD(P)H and FAD) was then measured within the oocyte.

In the absence of BMP15 (control), there were no significant differences in oocyte NAD(P)H auto-fluorescence intensity between 0 and 1 mM oxalomalate treatments (**Figure 2A**). COCs cultured in the presence of BMP15 had significantly higher intra-oocyte NAD(P)H intensity compared to the control groups. In contrast, intensity was significantly lower and at similar levels to the control groups in oocytes exposed to BMP15 and 1 mM oxalomalate ($P < 0.05$; **Figure 2A**).

A similar pattern of fluorescence intensity was seen for FAD, with the control groups having similar intensities regardless of oxalomalate treatment (**Figure 2B**). The significant increase in FAD intensity in the presence of BMP15 ($P < 0.05$) was reversed in the presence of 1 mM oxalomalate. Hence, oxalomalate treatment reduced the BMP15-mediated increases in NAD(P)H and FAD, most likely through reduced TCA cycle activity, suggesting the TCA cycle is a major source of NADPH within BMP15-treated oocytes.

Experiment 3: Intra-oocyte reduced glutathione (GSH), mitochondrial activity and reactive oxygen species (ROS) levels

Following 23 h cultures in the presence or absence of FSH and BMP15, COCs were labelled with monochlorobimane (MCB; for GSH determination), peroxyfluor 1 (PF1; for H_2O_2 determination) and Mitotracker Red CMXROS (active mitochondria) to determine if the presence of FSH and BMP15 influenced mitochondrial activity and localisation, cellular stress in the form of ROS (H_2O_2) and endogenous anti-oxidation protection in the form of GSH. In COCs cultured in the presence of FSH alone, there was a significant decrease in the mean intensity of intra-oocyte MCB compared to all the other treatment groups (MCB reflecting GSH levels; **Figure 3A&D,** $P < 0.001$**)**. In comparison, positive staining for active mitochondria was significantly higher within oocytes exposed to FSH during IVM, compared to the control group (Mitotracker Red as a measure for active mitochondria; **Figure 3B&D, $P < 0.05$**). Alone, BMP15 and FSH significantly increased PF1 levels, compare to the control but not the +FSH +BMP15 group (PF1 determines H_2O_2; **Figure 3C&D**).

To resolve whether BMP15 and FSH supplementation during IVM influenced the localisation of GSH, H_2O_2 and active mitochondria within the oocyte, image texure analyses (with the help of

grey-level co-occurrence matrices, GLCM) were performed. Higher values of textural features indicate higher levels of roughness/unevenness and reduced uniformity of positive staining. As similar patterns of localisation were seen for the angular secondary moment (ASM, the texture of the whole oocyte), contrast (sub-cellular/organelle texture) and correlation (relationships between neighbouring pixels); the ASM data is presented in **Figure 4**, with the remaining texture data presented in **Supplementary Figure S2**

There were no significant differences in the texture patterns of MCB positive staining (representing GSH) across treatments, with large variations in patterns seen within all groups (**Figure 4A,** $P > 0.05$). However, with both PF1 (representing H_2O_2) and Mitotracker Red localisation, BMP15 supplementation resulted in significantly lower texture values, hence smoother patterns of positive staining (main effect of BMP15; Mitotracker Red $P = 0.005$ and PF1; $P = 0.003$). Furthermore, BMP15 supplementation resulted in more consistent texture feature values within the Mitotracker Red and PF1 staining compared to the control group, which had large variations in texture values, as indicated by the SEM bars (**Figures 4B&C**).

In summary, FSH-stimulation reduced levels of GSH-positive staining within oocytes and increased mitochondrial activity and production of ROS in the form of H_2O_2. ROS-levels were also higher in BMP15-treated oocytes, regardless of the presence or absence of FSH. Furthermore, BMP15-treatment also promoted a more uniform localisation of mitochondrial localisation.

Experiment 4: Gene expression within the oocyte and cumulus vestment

The gene expression of key enzymes involved in glutathione synthesis and cycling, such as glutathione biosynthesis (*GSS*), reduction (*GSR, GSTA1*) and oxidation (*GPX1, GPX4*) were

measured in cumulus cells (CC) and COC-derived denuded oocytes (CDO) following 23 h IVM in the presence or absence of BMP15 and FSH. In both CC and CDO, there were no differences between treatments in regards to expression of glutathione synthesising (*GSS*, **Figure 5A&B**) and oxidising enzymes (GPX1 and GPX4, **Figure 5G-N**).

There were similar patterns of mRNA expression of *GSR* and *GSTA1*, enzymes involved in the reduction of glutathione, within the oocyte (CDO). FSH supplementation, regardless of the presence or absence of BMP15, significantly reduced gene expression compared to the control group (main effect, **Figure 5D&F,** $P < 0.05$). Furthermore, *GSTA1* was differentially expressed in cumulus cells, with significantly higher levels in +FSH alone compared to +BMP15; the opposite of what was seen in CDO (**Figure 5E**, $P < 0.05$).

Therefore, while FSH and BMP15 did not affect the expression of genes involved in glutathione synthesis and oxidation, FSH treatment significantly influenced glutathione cycling by decreasing the gene expression of enzymes involved in the reduction of glutathione.

Experiment 5: Amino acid turnover by intact cumulus oocyte complexes

Amino acid turnover was measured in spent media from the final 4 h of IVM of individual COCs in the presence or absence of FSH and BMP15 as a marker of developmental competence. There were no significant differences in total, essential and non-essential amino acid turnover between treatments (**Table 1**).

Isoleucine, serine and glutamine were the only amino acids that were consumed by COCs, with all other measured amino acid produced by COCs (**Figure 6**). Significant differences in glutamine turnover were observed (**Figure 6**), with the control group (-FSH –BMP15) producing

glutamine, compared to its consumption in the other treatment groups (-FSH -BMP15 = 16.4 ± 23.4 vs. +FSH +BMP15 = -75.0 ± 16.5 pmol/COC/h; $P < 0.05$). Alanine turnover was also >2-fold higher in the +FSH and +FSH +BMP15 groups compared to the control group (**Figure 6**; main effect of FSH, $P < 0.05$).

DISCUSSION

The addition of native OSF to oocyte maturation media through co-culture with denuded oocytes, or addition of recombinant OSFs improves oocyte developmental competence, on-time embryo development rates and fetal survival post-embryo transfer (Hussein et al. 2006; Yeo et al. 2008; Hussein et al. 2011; Sudiman et al. 2014), possibly overcoming a deficiency in endogenous OSF production during IVM (Mester et al. 2014). We have previously demonstrated that the addition of recombinant, pro-mature BMP15 results in an altered metabolic profile to COCs exposed to FSH (the most widely used media additive during IVM which stimulates COC metabolism and oocyte developmental competence) or the combination of FSH and BMP15 (Sutton-McDowall et al. 2012). COCs cultured with BMP15 alone demonstrate a preference for oxidative metabolism, with less glucose metabolised via glycolysis and significant increases in intra-oocyte FAD (**Figure 7**). Increased levels of NAD(P)H levels within the oocyte are also seen, without changing the REDOX ratio between treatment groups. Hence the aim of this study was to investigate the source of the increased NAD(P)H levels following culture in the presence of BMP15 and how this increase may be contributing to improved oocyte health, such as mitochondrial activity and the ability to deal with cellular stress.

We hypothesised that the increase in oocyte NAD(P)H was attributed to increased NADPH production. Numerous studies have suggested that a major source of NADPH production within

the oocyte is via glucose metabolism by G6PDH, within the oxidative arm of the pentose phosphate pathway (Downs et al. 1998; Urner and Sakkas 2005). Brilliant cresyl blue (BCB) is metabolised by G6PDH (hence BCB negative oocytes indicate active G6PDH) and has been used to predict the developmental competence of immature oocytes prior to IVM (Roca et al. 1998; Alm et al. 2005; Bhojwani et al. 2007). We exposed mature COCs to BCB following IVM with BMP15 and FSH to determined G6PDH activity. BMP15 supplementation resulted in lower proportions of BCB- oocytes, suggesting lower G6PDH and oxidative pentose phosphate pathway activity with BMP15 supplementation. In contrast, inhibiting IDH (TCA cycle) reduced the BMP15 stimulation of NAD(P)H auto-fluorescence, suggesting that a significant source of intra-oocyte NADPH is via the TCA-cycle, and BMP15 stimulation increases intra-oocyte TCA cycle activity. This is supported by Dumollard and colleagues (Dumollard et al. 2007b), who proposed that TCA cycle activity, especially IDH, contributes significantly to the intracellular REDOX potential in mouse oocytes.

A major role of NADPH is the recycling of GSSG to GSH, allowing the cell to respond to oxidative stresses, such as H_2O_2 derived from oxidative phosphorylation within the mitochondria. FSH-stimulation (in the absence of BMP15) reduced the intensity of MCB staining within the oocyte, suggesting lower intra-oocyte levels of GSH, while BMP15 supplementation (+FSH +BMP15) recovered MCB intensity. This concurs with the reduced gene expression of enzymes involved in the reduction of GSSG to GSH, namely *GSR* and *GSTA1*, within the oocyte following FSH stimulation. This suggests FSH stimulation reduces the ability for oocytes to regulate H_2O_2 levels through the reduction of GSSG to GSH. The increase in blastocyst development following IVM in the presence of both FSH and BMP15 observed in previous studies (Sutton-McDowall et al. 2012) may be attributed to the BMP15-induced increases in NADPH enabling a recovery of GSH levels.

The influence of BMP15 supplementation on oocyte and cumulus metabolism appears to vary with co-supplementation with different hormones and growth factors. The metabolism of oocytectomized complexes (intact COCs, in which the ooplasm has been surgically removed) did not differ from intact COCs or oocytectomized complexes co-cultured with denuded oocytes (Sutton et al. 2003), most likely due to FSH masking the stimulatory effects of BMP15 and other OSFs. More recently, EGF-like peptide amphiregulin supplementation with BMP15 further increases oocyte FAD and NAD(P)H (Sugimura et al. 2014), as opposed to the depression seen here with FSH-stimulation (Sutton-McDowall et al. 2012).

FSH was used in the current study as it is a widely used addition to cattle IVM systems to stimulate maturation and other cellular activities such as glucose metabolism (Sutton-McDowall et al. 2010). However, it is becoming increasingly evident that alternative hormones and growth factors should be explored for use in IVM systems, given the potential for increased cellular stress induced by FSH in the current study. As mentioned above, EGF-like peptides are ideal candidates given their addition improves development competence by prolonging gap junction communication between the oocyte and cumulus cells (Sugimura et al. 2014) and stimulation of glucose metabolism and cumulus expansion in mouse COCs (Richani et al. 2014).

In addition to measuring mean fluorescence intensity of MCB, Mitotracker Red and PF1, the texture of staining (grey-level co-occurrence matrices) were assessed as an indicator of the localisation and uniformity of positive fluorescence staining. Mitochondria synthesis occurs during oocyte development and remains static until implantation. In addition to copy number, mitochondrial distribution within the oocyte is constantly changing in response to energy expensive events such as meiotic progression (Van Blerkom 2009) and activity is largely

325 influenced by location (Diaz et al. 1999). Immature oocytes (germinal vesicle stage)
326 demonstrate a cortical pattern of mitochondrial localisation, verses a more disperse, even
327 distribution in mature (metaphase II, MII) oocytes (Dumollard et al. 2007a). However, clustering
328 or uneven distribution within MII oocytes is associated with compromised developmental
329 competence (Van Blerkom 2009). In the current study, BMP15 supplementation resulted in
330 "smoother" and more homogenous localisation of both Mitotracker Red and PF1 staining within
331 mature oocytes, regardless of FSH-stimulation. Furthermore, there was less variation in texture
332 within the +BMP15 and +BMP15 +FSH treatment groups, in particular compared to the –
333 BMP15 –FSH group. This suggests BMP15 supplementation during IVM is promoting an even
334 distribution of active mitochondria, contributing to improved function and developmental
335 competence.
336
337 A unique aspect of this study was the use of fluorescence probes in single, live oocytes to
338 investigate cellular metabolism. Where traditional enzymatic assays require pooling large
339 numbers of COCs/oocytes for the assessment of single enzymes, in the current study
340 fluorescence probes were used determine the level and localisation of reactive oxygen species,
341 anti-oxidants (specifically H_2O_2 and GSH) and active mitochondria within the oocyte following
342 the culture of intact COCs in the presence of BMP15 and FSH. This technique allowed the
343 creation of a profile of three metabolic outcomes; with positive staining indicating levels of
344 enzymatic activity, localisation and textural patterning, within single live oocytes, vs. large
345 numbers of pooled oocytes for traditional enzymatic assays. The use of quantitative texture
346 analyses further enhanced the interpretation of imaging data. Grey-level co-occurrence
347 matrices (GLCM) have been extensively utilised in diagnostic imaging (Castellano et al. 2004)
348 and applied in dermatology (Mittra and Parekh 2011), liver (Losa and Castelli 2005) and cancer

349 imaging (Alvarenga et al. 2007). To our knowledge, this is the first study to present the results
350 of such image analyses to investigate patterns of metabolism within oocytes.
351
352 Differences in amino acid profiles of oocytes denuded of their cumulus vestment compared to
353 intact COCs are highlighted by a recent study of oocyte metabolism during the final 6 h of IVM
354 (Hemmings et al. 2012). Cattle oocytes that underwent successful fertilisation, cleavage and
355 developed to the blastocyst stage (on-time embryo development) had lower glutamine uptake
356 and alanine appearance in media compared to incompetent oocytes (uncleaved following
357 fertilisation) (Hemmings et al. 2012). Likewise, in the current study, glutamine and alanine were
358 influenced by treatments. Glutamine consumption and alanine production was significantly
359 higher in COCs that were incubated with treatments that resulted in improved oocyte
360 developmental competence. Both glutamine and alanine are involved in carbohydrate
361 metabolism, with high levels of glutamine consumption seen in pre-cancerous and cancerous
362 cells (Varone et al. 2014) and alanine is involved in ammonium detoxification (Schliess et al.
363 2014). Alanine production was highest in the FSH treatment groups (regardless of BMP15),
364 both of which had the highest levels of glycolytic activity (Sutton-McDowall et al. 2012). Indeed,
365 a recent study demonstrated a link between alanine and glutamine levels in follicular fluid and
366 developmental competence of oocytes (Matoba et al. 2014).
367
368 Both glutamine metabolism and pyruvate oxidation within cattle oocyte significantly increased
369 towards the end of maturation as measured in denuded oocytes following COC maturation
370 using radiolabelled substrates (Rieger and Loskutoff 1994; Steeves and Gardner 1999).
371 Therefore, it seems reasonable to suggest that within treatments impacting oxidative
372 phosphorylation, such as the addition of BMP15, greater levels of glutamine are also
373 metabolised within the oocyte. However, we did not assess this directly in the current study.

In conclusion, we found that BMP15 supplementation during bovine oocyte IVM stimulates NADPH production via IDH and the TCA cycle within the oocyte, rather than G6PDH (pentose phosphate pathway), further supporting the role of BMP15 in inducing oxidative metabolism within the oocyte. Furthermore, BMP15 supplementation (regardless of FSH) promoted a more homogenous and consistent localisation of active mitochondria, indicative of improved developmental competence. FSH reduces GSH-levels within the oocyte, corresponding with reduced gene expression of glutathione reducing enzymes. The combination of both FSH and BMP15 significantly increased glutamine consumption, consistent with increased oxidative metabolism. Hence, significant increases in oocyte developmental competence previously reported is likely to due the combination of FSH and BMP15 resulting in equilibration of metabolism within the oocyte, rather than a preference for oxidative or reductive metabolism; for example, FSH stimulated glucose metabolism within the cumulus vestment, while BMP15 promoted oxidative phosphorylation through improved mitochondrial function and protection against cellular stress, through increased NADPH production promoting improved glutathione recycling.

MATERIALS AND METHODS

Unless stated, all chemicals were obtained from Sigma Aldrich (St Louis, MO).

Oocyte collection and in vitro maturation (IVM)

Cattle ovaries were collected from a local abattoir (T&R, Murray Bridge, South Australia) and transported to the laboratory in warm saline (30-35°C). Immature COCs were aspirated from ovarian follicles using an 18-gauge needle and a 10 ml syringe, in undiluted follicular fluid. Compact COCs with intact cumulus vestments, with at least three cell layers and un-granulated

399 ooplasms were selected in undiluted follicular fluid, washed once in IVM medium and then
400 transferred into the corresponding IVM treatments. The IVM media was bicarbonate buffered
401 TCM199 (ICN Biochemicals; Irvine, CA USA) + 0.5 mM pyruvate + 4 mg/ml fatty acid free
402 (FAF) BSA (ICPBio Ltd; Auckland, New Zealand) ± 100 mIU/ml FSH (Puregon; Organon, Oss,
403 Netherlands) ± 100 ng/ml BMP15, a concentrated preparation of recombinant human BMP15
404 pro/mature complex produced in our laboratory using 293T cells, as previously described
405 (Pulkki et al. 2011; Mottershead et al. 2012). Groups of 10 COCs were cultured in 100 µl of pre-
406 equilibrated IVM media, overlaid with paraffin oil (Merck; Darmstadt, Germany) at 38.5°C in 6%
407 CO_2 in humidified air. Unless otherwise stated, COCs were cultured for 23 h.
408
409 ***Experiment 1: Intra-oocyte glucose 6-phosphate dehydrogenase (G6PDH) activity***
410 After 21.5 h of culture ± FSH ± BMP15, COCs were transferred into fresh IVM media + 23 µM
411 brilliant cresyl blue (BCB) and cultured for 90 mins at 38.5°C. At the completion of culture,
412 COCs were washed once in wash medium (VitroWash; IVF Vet Solutions, Adelaide, Australia +
413 4 mg/ml FAF BSA) and staining of the oocyte was assessed using a dissecting microscope.
414 BCB is readily metabolised by G6PDH, hence blue oocytes (BCB^+) arise from COCs with low
415 G6PDH activity and BCB^- oocytes from COCs with high G6PDH activity. Data are presented as
416 the proportion of BCB negative (-) oocytes from the total oocyte pool for each treatment and
417 replicate. Four replicate experiments were performed with 20-30 COCs used within each
418 treatment group and replicate.
419
420 ***Experiment 2: Intra-oocyte isocitrate dehydrogenase (IDH) activity and NAD(P)H levels***
421 Following 23 h of culture in IVM media without FSH ± 100 ng/ml BMP15, COCs were
422 transferred into VitroWash + 4 mg/ml FAF BSA and 0 or 1 mM oxalomalate (an inhibitor of
423 IDH). A dose response of oxalomalate revealed that media containing 2 mM oxalomalate or

higher had high levels of background fluorescence; hence 1 mM oxalomalate was used in subsequent experiments (**Supplementary Figure S1**). COCs were transferred in 5 µl of corresponding wash medium (± oxalomalate), overlaid with oil in glass bottom confocal dishes (Cell E&G; Houston, TX, USA). Auto-fluorescence images were captured for live oocytes, using the FluoView FV10i confocal microscope and accompanying software (Olympus; Tokyo, Japan), measuring green (FAD; excitation = 473 nm and emission = 490-590 nm) and blue (NADH/NADPH = NAD(P)H; excitation = 405 nm and emission = 420-520 nm) emissions using inbuilt filters. Microscope settings such as laser intensity and image size were kept constant. Quantification of the fluorescence intensity was determined using Image J imaging software (NIH; Bethesda, MD, USA), with the raw data normalised to fluorescence beads (InSpeck, Molecular Probes; Eugene, OR, USA). Three replicate experiments were performed with 10 COCs measured per treatment group, per replicate.

Experiment 3: Intra-oocyte reduced glutathione (GSH), mitochondrial activity and reactive oxygen species (ROS) levels

After 23 h of culture, COCs were denuded by repeat pipetting and transferred into VitroWash + 4 mg/ml FAF BSA + 20 µM peroxyfluor-1 (PF1) for 1 h; 12.5 µM monochlorobimane (MCB) for 30 mins and 200 nM Mitotracker Red CMXROS (Molecular Probes) for 15 mins at 38.5°C, in darkness. Oocytes were washed once in VitroWash + 4 mg/ml FAF BSA and transferred into 2 µl smears of wash medium in glass bottom confocal dishes.

PF1 is an aryl boronate probe that fluoresces on reaction with H_2O_2 (Chang et al. 2004). It has higher specificity for H_2O_2 and peroxynitrite over other ROS, unlike commonly used non-specific ROS probes such as 2',7'-dichlorohydrofluorescein diacetate (H_2DCFDA). H_2DCFDA also autoxidizes and catalyzes superoxide production, leading to false positive fluorescence

(Murphy et al. 2011). PF1 was prepared using microwave irradiation in place of conventional heating: 3',6'-diiodofluoran (Chang et al. 2004) (89 mg, 0.16 mmol), bis(pinacolato)diboron (160 mg, 0.63 mmol), potassium acetate (141 mg, 0.63 mmol) and Pd(dppf)Cl_2 (14 mg, 0.02 mmol) were pre- dried in vacuo, dissolved in DMF (4 ml) under N_2 atmosphere in a sealed microwave vial fitted with a teflon cap. The light brown mixture was reacted in a CEM Discover microwave synthesiser (Matthews, NC) at 80 °C for 2 h. The solvent was removed under reduced pressure to give a dark brown powder which was purified by column chromatography eluting with 4:1 hexane:ethyl acetate to give PF1 as a white solid. (40 mg, 45%); ^{1}HNMR ($CDCl_3$, 300MHz): δ(ppm) 8.03 (1H, m), 7.74 (2H, s), 7.60 (2H, m), 7.43 (2H, dd, J_1=7.8Hz, J_2=1.1Hz), 7.06 (1H, m), 6.86 (2H, d, J=7.8Hz), 1.35 (24H, s).

Both MCB and Mitotracker Red CMXROS are commercially available fluorescent probes. MCB fluoresces when bound to low weight thiol compounds, with the highest affinity for reduced glutathione (GSH), representing 99% of the intracellular fluorescence intensity (Keelan et al. 2001). Mitotracker Red CMXROS accumulates within mitochondria, depending on membrane potential.

Intra-oocyte fluorescence was captured using the Fluoview FV10i confocal microscopy (MCB: excitation = 358 nm and emission = 461 nm; PF1: excitation = 496 nm and emission = 519; Mitotracker Red: excitation = 578 nm and emission = 598) with laser, magnification and image settings remaining constant across replicates.

Image processing and analyses were performed using Image J software and the plugin/macro option, hence allowing for semi-automated analyses. Macros for image file processing and measurements are included as **supplementary data.** Briefly, using Macro 1 (**supplementary**

474 **data**), individual images were captured, representing each fluorescent channel, and then
475 converted from Olympus confocal image files (Olympus image format, oif) into 8-bit grey scale
476 tiff files. The oocyte was selected as a region of interest (ROI) and the background of the image
477 was excluded. Mean intensity (Macro 2, **supplementary data**) and selected texture features
478 analyses (grey-level co-occurrence matrices, GLCM, Macro 3) of the ROI were performed.
479 Macros 2 and 3 are available from the NIH Image J website (http://rsb.info.nih.gov/ij/plugins).
480 GLCM analysis was applied to determine differences in the localisation of fluorescence
481 intensity, hence the texture (uniformity/smoothness/roughness) of staining patterns (Haralick et
482 al. 1973; Murata et al. 2001; Cabrera 2006). Angular secondary moment (ASM) represents the
483 texture of the whole oocyte, contrast represents the texture of sub-cellular organelles and
484 correlation represents intensity differences between pixels. A total of 10 COCs used per
485 treatment.
486
487 The relationship between MCB fluorescence and intra-oocyte GSH levels was validated by
488 incubating COCs in buthionine sulphoximine (BSO), an inhibitor of the first stage of glutathione
489 synthesis (gamma-glutamylcysteinesynthetase). Groups of 10 COCs were cultured in VitroMat
490 + 4 mg/ml FAF BSA + 0.1 IU/ml FSH and 0, 1, 2, 5 and 10 mM BSO. After 23 h of culture,
491 COCs were incubated with 12.5 μM MCB (as above) and fluorescence intensity was
492 determined within denuded oocytes. Results of the dose response are present in
493 **Supplementary Figure S3**. Two replicate experiments were performed, with 10 COCs per
494 replicate.
495
496 ***Experiment 4: Gene expression within the oocyte and cumulus vestment***
497 Total RNA from 50 COC-derived oocytes (CDO) or the cumulus cells (CC) from 50 COCs was
498 isolated using Trizol according to manufacturer's instructions (Life Technologies; Mulgrave,

VIC, Australia). Total RNA was treated with 1 IU DNAse (Life Technologies) at 37°C for 1 h as per manufacturer's instructions. First strand complementary DNA (cDNA) was synthesised using random hexamer primers and Superscript III reverse transcriptase (Life Technologies). Gene primers for Real Time RT-PCR were designed against published mRNA sequences from the NCBI Pubmed Database using Primer 3 software (**Table 2**) and synthesised by Geneworks (Geneworks, Adelaide, SA, Australia). Real time RT-PCR was performed in triplicate for each sample on a Rotor-Gene™ 6000 (Corbett Life Science; Sydney, NSW, Australia). In each reaction, cDNA from 10ng total RNA, 0.1 l forward and reverse primers and 10 l SYBR ® Green Master Mix (Applied Biosystems; CA, USA), and water was added to a final volume of 10 l. All primers were used at an optimised concentration of 25 M. PCR conditions were as follows: 50°C for 2 min, 95°C for 10 min, followed by 40 cycles of 95°C for 15 sec and 60°C for 60 sec. Single product amplification was confirmed by analysis of disassociation curves and ethidium bromide stained agarose gel electrophoresis. Controls included the absence of cDNA template or the reverse transcriptase enzyme and each showed no evidence of product amplification or genomic DNA contamination. All gene expression was normalised to an *RPL19* (*L19*) internal loading control that was amplified in parallel for each sample. Results were then expressed as a raw expression value using the $2^{-(\Delta\Delta CT)}$ method.

Experiment 5: Amino acid turnover by intact cumulus oocyte complexes

Groups of 10 COCs were cultured ± FSH ± BMP15. After 19 h of culture, individual COCs were transferred into 2 µl drops of fresh culture medium and cultured for 4 h. At the completion of the culture period, the COC was removed, 1 µl of the spent medium was transferred into a 1.7 ml eppendorf tube, snap frozen, freeze dried and stored at -80°C. In addition, for each treatment and replicate a drop of media without a COC was cultured simultaneously to account for amino acid concentrations within the media.

524

525 Freeze dried samples were analysed for amino acid composition using a protocol similar to
526 (Wale and Gardner 2012). Amino acid analysis was undertaken using the derivatization-
527 labeling reagent 6-aminoquinolyl-N-hydroxysuccinimidyl carbamate (Aqc) and a triple-
528 quadrupole mass spectrometer (LC-QqQ-MS), to facilitate the concentrations of co-eluted
529 fractions of a variety of amines to be resolved and quantitated by comparison against a
530 standard calibration curve. A 2.5 mM stock solution of amino acids was prepared containing
531 the following; lysine, histidine, asparagine, arginine, taurine, serine, glutamine, glycine,
532 aspartate, glutamate, threonine, alanine, proline, cysteine, tyrosine, methionine, valine,
533 isoleucine, leucine, phenylalanine and tryptophan. Calibration standards for these amino acids
534 were then prepared by diluting the stock solution to 150, 100, 50, 25, 10, 5, 1, 0.5, 0.1, 0.05,
535 and 0.01 µM in water using volumetric glassware. Norleucine was used as an internal standard
536 in borate buffer containing the antioxidant ascorbic acid and the reducing agent tris(2-
537 carboxyethyl)phosphine. Each dried media sample, including a control media sample not used
538 for COC incubation, was resuspended in 10 µL of MilliQ water and 10 µl aliquots of each amino
539 acid standard prepared. To all standards and samples, 70 µl of borate buffer was then added
540 and mixed by vortex for 20 sec followed by centrifugation (1 min). To each 80 µl volume, 20 µl
541 of Aqc was added and the solution, vortexed immediately for 20 sec, and warmed on a heating
542 block (Thermomixer, Eppendorf) with shaking (1000 rpm) for 10 min at 55°C. The final solution
543 was then allowed to cool to ambient temperature before centrifugation (1 min), followed by
544 analysis using an Agilent 1200 LC-system coupled to an Agilent 6420 ESI-QqQ-MS (Santa
545 Clara, CA).

546

547 The amino acid concentrations in spent media were normalised against a drop of media that
548 had been cultured without a COC and consumption/production were calculated as pmol per

549 COC per hour of culture (4 h). A negative value indicates net depletion/consumption, with
550 positive values representing production/appearance in the COC media samples. Four
551 experimental replicates were performed, with the spent media from two individual COC cultures
552 collected per treatment group, within replicates.
553
554 ***Statistical analyses***
555 Differences between treatments were determined using a general linear model, with BMP15
556 and FSH as main effects with the exception of experiment 2, in which the main effects were
557 BMP15 and oxalomalate. Differences between individual treatment groups were determined
558 using the Bonferroni post-hoc test. Proportional data was arcsine transformed prior to analysis.
559 All statistical tests were performed using SPSS version 22 statistical software and P-values
560 less than 0.05 were considered statistically significant.
561
562 **ACKNOWLEDGEMENTS**
563 The authors would like to thank SEMEX Pty Ltd Australia for the kind gift of bull semen. This
564 study was funded by National Health and Medical Research Council Australia Project
565 (1008137) and Development (1017484) Grants and a collaborative research grant from Cook
566 Medical (Eight Mile Plains, QLD Australia). The Fluoview FV10i confocal microscope was
567 purchased as part of the Sensing Technologies for Advanced Reproductive Research (STARR)
568 facility, funded by the South Australia's Premier's Science and Research Fund. The authors
569 declare no conflict of interest.
570
571 **REFERENCES**
572 Albertini DF, Combelles CM, Benecchi E, Carabatsos MJ. 2001. Cellular basis for paracrine
573 regulation of ovarian follicle development. Reproduction 121(5):647-653.

574 Alm H, Torner H, Lohrke B, Viergutz T, Ghoneim IM, Kanitz W. 2005. Bovine blastocyst
575 development rate in vitro is influenced by selection of oocytes by brillant cresyl blue
576 staining before IVM as indicator for glucose-6-phosphate dehydrogenase activity.
577 Theriogenology 63(8):2194-2205.
578 Alvarenga AV, Pereira WC, Infantosi AF, Azevedo CM. 2007. Complexity curve and grey level
579 co-occurrence matrix in the texture evaluation of breast tumor on ultrasound images.
580 Medical physics 34(2):379-387.
581 Bhojwani S, Alm H, Torner H, Kanitz W, Poehland R. 2007. Selection of developmentally
582 competent oocytes through brilliant cresyl blue stain enhances blastocyst development
583 rate after bovine nuclear transfer. Theriogenology 67(2):341-345.
584 Buccione R, Schroeder AC, Eppig JJ. 1990a. Interactions between somatic cells and germ
585 cells throughout mammalian oogenesis. Biol Reprod 43(4):543-547.
586 Buccione R, Vanderhyden BC, Caron PJ, Eppig JJ. 1990b. FSH-induced expansion of the
587 mouse cumulus oophorus in vitro is dependent upon a specific factor(s) secreted by
588 the oocyte. Dev Biol 138(1):16-25.
589 Cabrera JE. 2006. Texture Analyzer. V0.4 ed.
590 Castellano G, Bonilha L, Li LM, Cendes F. 2004. Texture analysis of medical images. Clinical
591 radiology 59(12):1061-1069.
592 Cetica P, Pintos L, Dalvit G, Beconi M. 2003. Involvement of enzymes of amino acid
593 metabolism and tricarboxylic acid cycle in bovine oocyte maturation in vitro.
594 Reproduction 126(6):753-763.
595 Chance B, Schoener B, Oshino R, Itshak F, Nakase Y. 1979. Oxidation-reduction ratio studies
596 of mitochondria in freeze-trapped samples. NADH and flavoprotein fluorescence
597 signals. The Journal of biological chemistry 254(11):4764-4771.

598 Chang MC, Pralle A, Isacoff EY, Chang CJ. 2004. A selective, cell-permeable optical probe for
599 hydrogen peroxide in living cells. Journal of the American Chemical Society
600 126(47):15392-15393.
601 Crawford JL, McNatty KP. 2012. The ratio of growth differentiation factor 9: bone
602 morphogenetic protein 15 mRNA expression is tightly co-regulated and differs between
603 species over a wide range of ovulation rates. Mol Cell Endocrinol 348(1):339-343.
604 de Matos DG, Furnus CC, Moses DF, Baldassarre H. 1995. Effect of cysteamine on glutathione
605 level and developmental capacity of bovine oocyte matured in vitro. Molecular
606 Reproduction and Development 42(4):432-436.
607 Diaz G, Setzu MD, Zucca A, Isola R, Diana A, Murru R, Sogos V, Gremo F. 1999. Subcellular
608 heterogeneity of mitochondrial membrane potential: relationship with organelle
609 distribution and intercellular contacts in normal, hypoxic and apoptotic cells. J Cell Sci
610 112 (Pt 7):1077-1084.
611 Downs SM, Humpherson PG, Leese HJ. 1998. Meiotic induction in cumulus cell-enclosed
612 mouse oocytes: involvement of the pentose phosphate pathway. Biol Reprod
613 58(4):1084-1094.
614 Dumollard R, Duchen M, Carroll J. 2007a. The role of mitochondrial function in the oocyte and
615 embryo. Current topics in developmental biology 77:21-49.
616 Dumollard R, Ward Z, Carroll J, Duchen MR. 2007b. Regulation of redox metabolism in the
617 mouse oocyte and embryo. Development 134(3):455-465.
618 Haralick RM, Shanmuga.K, Dinstein I. 1973. Textural Features for Image Classification. Ieee T
619 Syst Man Cyb Smc3(6):610-621.
620 Hemmings KE, Leese HJ, Picton HM. 2012. Amino acid turnover by bovine oocytes provides
621 an index of oocyte developmental competence in vitro. Biol Reprod 86(5):165, 161-
622 112.

623 Hussein TS, Froiland DA, Amato F, Thompson JG, Gilchrist RB. 2005. Oocytes prevent
624 cumulus cell apoptosis by maintaining a morphogenic paracrine gradient of bone
625 morphogenetic proteins. J Cell Sci 118(Pt 22):5257-5268.
626 Hussein TS, Sutton-McDowall ML, Gilchrist RB, Thompson JG. 2011. Temporal effects of
627 exogenous oocyte-secreted factors on bovine oocyte developmental competence
628 during IVM. Reprod Fertil Dev 23(4):576-584.
629 Hussein TS, Thompson JG, Gilchrist RB. 2006. Oocyte-secreted factors enhance oocyte
630 developmental competence. Dev Biol 296(2):514-521.
631 Keelan J, Allen NJ, Antcliffe D, Pal S, Duchen MR. 2001. Quantitative imaging of glutathione in
632 hippocampal neurons and glia in culture using monochlorobimane. J Neurosci Res
633 66(5):873-884.
634 Krisher R. 2013. In vivo and in vitro environmental effects on mammalian oocyte quality. Ann
635 Rev Anim Biosci.
636 Larsen WJ, Wert SE. 1988. Roles of cell junctions in gametogenesis and in early embryonic
637 development. Tissue and Cell 20(6):809-848.
638 Li R, Norman RJ, Armstrong DT, Gilchrist RB. 2000. Oocyte-secreted factor(s) determine
639 functional differences between bovine mural granulosa cells and cumulus cells. Biol
640 Reprod 63(3):839-845.
641 Losa GA, Castelli C. 2005. Nuclear patterns of human breast cancer cells during apoptosis:
642 characterisation by fractal dimension and co-occurrence matrix statistics. Cell and
643 tissue research 322(2):257-267.
644 Matoba S, Bender K, Fahey AG, Mamo S, Brennan L, Lonergan P, Fair T. 2014. Predictive
645 value of bovine follicular components as markers of oocyte developmental potential.
646 Reprod Fertil Dev 26(2):337-345.

647 Matzuk MM, Burns KH, Viveiros MM, Eppig JJ. 2002. Intercellular communication in the
648 mammalian ovary: oocytes carry the conversation. Science 296(5576):2178-2180.
649 Mayevsky A, Chance B. 1982. Intracellular oxidation-reduction state measured in situ by a
650 multichannel fiber-optic surface fluorometer. Science 217(4559):537-540.
651 Mester B, Ritter LJ, Pitman JL, Bibby AH, Gilchrist RB, McNatty KP, Juengel JL, McIntosh CJ.
652 2014. Oocyte expression, secretion and somatic cell interaction of mouse bone
653 morphogenetic protein 15 during the peri-ovulatory period. Reproduction, fertility, and
654 development.
655 Mittra AK, Parekh R. 2011. Automated detection of skin diseases using texture features.
656 Interational Journal of Engineering Science and Technology 3(6):4801-4808.
657 Mottershead DG, Ritter LJ, Gilchrist RB. 2012. Signalling pathways mediating specific
658 synergistic interactions between GDF9 and BMP15. Mol Hum Reprod 18(3):121-128.
659 Murata S, Herman P, Lakowicz JR. 2001. Texture analysis of fluorescence lifetime images of
660 AT- and GC-rich regions in nuclei. J Histochem Cytochem 49(11):1443-1451.
661 Murphy MP, Holmgren A, Larsson NG, Halliwell B, Chang CJ, Kalyanaraman B, Rhee SG,
662 Thornalley PJ, Partridge L, Gems D, Nystrom T, Belousov V, Schumacker PT,
663 Winterbourn CC. 2011. Unraveling the biological roles of reactive oxygen species. Cell
664 metabolism 13(4):361-366.
665 Pulkki MM, Myllymaa S, Pasternack A, Lun S, Ludlow H, Al-Qahtani A, Korchynskyi O, Groome
666 N, Juengel JL, Kalkkinen N, Laitinen M, Ritvos O, Mottershead DG. 2011. The
667 bioactivity of human bone morphogenetic protein-15 is sensitive to C-terminal
668 modification: characterization of the purified untagged processed mature region. Mol
669 Cell Endocrinol 332(1-2):106-115.

670 Richani D, Sutton-McDowall ML, Frank LA, Gilchrist RB, Thompson JG. 2014. Effect of
671 epidermal growth factor-like peptides on the metabolism of in vitro- matured mouse
672 oocytes and cumulus cells. Biol Reprod 90(3):49.
673 Rieger D, Loskutoff NM. 1994. Changes in the metabolism of glucose, pyruvate, glutamine and
674 glycine during maturation of cattle oocytes in vitro. J Reprod Fertil 100(1):257-262.
675 Roca J, Martinez E, Vazquez JM, Lucas X. 1998. Selection of immature pig oocytes for
676 homologous in vitro penetration assays with the brilliant cresyl blue test. Reprod Fertil
677 Dev 10(6):479-485.
678 Salhab M, Dhorne-Pollet S, Auclair S, Guyader-Joly C, Brisard D, Dalbies-Tran R, Dupont J,
679 Ponsart C, Mermillod P, Uzbekova S. 2013. In vitro maturation of oocytes alters gene
680 expression and signaling pathways in bovine cumulus cells. Molecular reproduction
681 and development 80(2):166-182.
682 Salhab M, Tosca L, Cabau C, Papillier P, Perreau C, Dupont J, Mermillod P, Uzbekova S.
683 2011. Kinetics of gene expression and signaling in bovine cumulus cells throughout
684 IVM in different mediums in relation to oocyte developmental competence, cumulus
685 apoptosis and progesterone secretion. Theriogenology 75(1):90-104.
686 Salustri A, Ulisse S, Yanagishita M, Hascall VC. 1990a. Hyaluronic acid synthesis by mural
687 granulosa cells and cumulus cells in vitro is selectively stimulated by a factor produced
688 by oocytes and by transforming growth factor-beta. J Biol Chem 265(32):19517-19523.
689 Salustri A, Yanagishita M, Hascall VC. 1990b. Mouse oocytes regulate hyaluronic acid
690 synthesis and mucification by FSH-stimulated cumulus cells. Dev Biol 138(1):26-32.
691 Sanchez MC, Sedo CA, Julianelli VL, Romanato M, Calvo L, Calvo JC, Fontana VA. 2013.
692 Dermatan sulfate synergizes with heparin in murine sperm chromatin decondensation.
693 Systems biology in reproductive medicine 59(2):82-90.

694 Schliess F, Hoehme S, Henkel SG, Ghallab A, Driesch D, Bottger J, Guthke R, Pfaff M,
695 Hengstler JG, Gebhardt R, Haussinger D, Drasdo D, Zellmer S. 2014. Integrated
696 metabolic spatial-temporal model for the prediction of ammonia detoxification during
697 liver damage and regeneration. Hepatology.
698 Skala M, Ramanujam N. 2010. Multiphoton redox ratio imaging for metabolic monitoring in vivo.
699 Methods Mol Biol 594:155-162.
700 Steeves TE, Gardner DK. 1999. Metabolism of glucose, pyruvate, and glutamine during the
701 maturation of oocytes derived from pre-pubertal and adult cows. Molecular
702 Reproduction and Development 54(1):92-101.
703 Su YQ, Wu X, O'Brien MJ, Pendola FL, Denegre JN, Matzuk MM, Eppig JJ. 2004. Synergistic
704 roles of BMP15 and GDF9 in the development and function of the oocyte-cumulus cell
705 complex in mice: genetic evidence for an oocyte-granulosa cell regulatory loop. Dev
706 Biol 276(1):64-73.
707 Sudiman J, Ritter LJ, Feil DK, Wang X, Chan K, Mottershead DG, Robertson DM, Thompson
708 JG, Gilchrist RB. 2014. Effects of differing oocyte-secreted factors during mouse in
709 vitro maturation on subsequent embryo and fetal development. Journal of assisted
710 reproduction and genetics 31(3):295-306.
711 Sugimura S, Ritter LJ, Sutton-McDowall ML, Mottershead DG, Thompson JG, Gilchrist RB.
712 2014. Amphiregulin co-operates with bone morphogenetic protein 15 to increase
713 bovine oocyte developmental competence: effects on gap junction-mediated
714 metabolite supply. Mol Hum Reprod.
715 Sutton ML, Cetica PD, Beconi MT, Kind KL, Gilchrist RB, Thompson JG. 2003a. Influence of
716 oocyte-secreted factors and culture duration on the metabolic activity of bovine
717 cumulus cell complexes. Reproduction 126(1):27-34.

718 Sutton ML, Gilchrist RB, Thompson JG. 2003b. Effects of in-vivo and in-vitro environments on
719 the metabolism of the cumulus-oocyte complex and its influence on oocyte
720 developmental capacity. Hum Reprod Update 9(1):35-48.
721 Sutton-McDowall M, Gilchrist R, Thompson J. 2010. The pivotal role of glucose metabolism in
722 determining oocyte developmental competence. Reproduction 139(4):685-695.
723 Sutton-McDowall ML, Mottershead DG, Gardner DK, Gilchrist RB, Thompson JG. 2012.
724 Metabolic differences in bovine cumulus-oocyte complexes matured in vitro in the
725 presence or absence of follicle-stimulating hormone and bone morphogenetic protein
726 15. Biol Reprod 87(4):87, 81-88.
727 Takahashi M, Nagai T, Hamano S, Kuwayama M, Okamura N, Okano A. 1993. Effect of thiol
728 compounds on in vitro development and intracellular glutathione content of bovine
729 embryos. Biol Reprod 49(2):228-232.
730 Urner F, Sakkas D. 2005. Involvement of the pentose phosphate pathway and redox regulation
731 in fertilization in the mouse. Mol Reprod Dev 70(4):494-503.
732 Van Blerkom J. 2009. Mitochondria in early mammalian development. Semin Cell Dev Biol
733 20(3):354-364.
734 Vanderhyden BC, Macdonald EA. 1998. Mouse oocytes regulate granulosa cell
735 steroidogenesis throughout follicular development. Biol Reprod 59(6):1296-1301.
736 Varone A, Xylas J, Quinn KP, Pouli D, Sridharan G, McLaughlin-Drubin ME, Alonzo C, Lee K,
737 Munger K, Georgakoudi I. 2014. Endogenous two-photon fluorescence imaging
738 elucidates metabolic changes related to enhanced glycolysis and glutamine
739 consumption in pre-cancerous epithelial tissues. Cancer Res.
740 Wale PL, Gardner DK. 2012. Oxygen regulates amino acid turnover and carbohydrate uptake
741 during the preimplantation period of mouse embryo development. Biol Reprod
742 87(1):24, 21-28.

743 Yeo CX, Gilchrist RB, Thompson JG, Lane M. 2008. Exogenous growth differentiation factor 9
744 in oocyte maturation media enhances subsequent embryo development and fetal
745 viability in mice. Hum Reprod 23(1):67-73.
746
747

748 **FIGURE AND TABLE LEGENDS**

749 **Figure 1.** The influence of FSH and BMP15 supplementation during oocyte maturation on
750 glucose 6-phosphate dehydrogenase activity, as determined by brilliant cresyl blue (BCB)
751 staining within the oocyte. Bars represent means + SEM and different superscripts indicate
752 significant differences (^{ab} $P < 0.05$).

753

754 **Figure 2**. Following 23 h of culture in the presence or absence of BMP15 (no FSH), COCs
755 were treated with oxalomalate (ox; an inhibitor of isocitrate dehydrogenase) and A) NAD(P)H
756 and B) FAD autofluorescence within the oocyte was measured. Bars represent means + SEM
757 and different superscripts indicate significant differences (^{ab} $P < 0.05$).

758

759 **Figure 3.** Anti-oxidants, mitochondrial activity and reactive oxygen species (ROS) levels within
760 oocytes following IVM in the presence of FSH and BMP, as indicated by the mean intensities of
761 A) monochloridebimane (MCB, reduced glutathione, GSH); B) mitotracker red (active
762 mitochondria) and C) peroxyfluor 1 (PF1, H_2O_2). Bars represent means + SEM and different
763 superscripts indicate significant differences (^{abc} $P < 0.05$). D) Representative images of the
764 positive staining. The scale bar = 50 μM.

765

766 **Figure 4.** Textural analyses, indicated by angular secondary moment, of anti-oxidants,
767 mitochondrial activity and reactive oxygen species (ROS) levels within oocytes following IVM in
768 the presence of FSH and BMP, as indicated by the textural values of A) monochloridebimane
769 (MCB, reduced glutathione, GSH); B) mitotracker red (active mitochondria) and C) peroxyfluor
770 1 (PF1, H_2O_2). Data points indicate individual oocytes, bars represent means $\pm$ SEM and
771 different superscripts indicate significant differences (^{ab} $P < 0.05$).

772

773 **Figure 5.** mRNA expression of enzymes involved in NADPH metabolism and glutathione. Intact
774 COCs were cultured in the presence or absence of BMP15 and FSH and separated into COC-
775 derived oocyte (CDO) and cumulus cells (CC). Bars represent means + SEM and different
776 superscripts indicate significant differences (^{ab} $P < 0.05$).
777
778 **Figure 6.** Amino acid turnover by intact COCs cultured in the presence and absence of FSH
779 and BMP15. Bars represent means + SEM and different superscripts indicate significant
780 differences (^{abxy} $P < 0.05$).
781
782 **Figure 7**. A summary of the changes in metabolism within the cumulus cells and oocytes
783 treated with FSH and BMP15. Previous studies have demonstrated that the presence of both
784 FSH and BMP15 during IVM significantly increased blastocyst development rates (total
785 blastocysts from cleaved) to 52% compared to 28% -FSH –BMP15, (Sutton-McDowall et al.
786 2012). Despite similar blastocyst development rates, when FSH and BMP15 were added
787 separately during IVM (+FSH = 44% and +BMP15 = 41%), different metabolic profiles were
788 observed in the COCs. The presence of FSH alone induces higher levels of glucose
789 metabolism within the cumulus cells via glycolysis and hexosamine biosynthetic pathway
790 (HBP), hence extra cellular matrix formation. Conversely, the presence of BMP15 alone
791 promotes higher levels of FAD and NADPH/NADH levels within the oocyte. In the current
792 study, BMP15 induced NADPH production via the TCA cycle. Furthermore, mitochondrial
793 localisation is more uniform in oocytes treated with BMP15. FSH-stimulated reduces GSH
794 levels and the gene expression of enzymes involved in glutathione reduction, compromising the
795 ability for oocytes to recycle glutathione in response to increased H_2O_2 production from
796 increased mitochondrial activity. BMP15 treatment also resulted in increased H_2O_2 production,

however, higher levels of GSH, NADPH and improved mitochondrial localisation could counteract this.

Supplementary Figure S1: Background fluorescence of oxalomalate using blue (ex = 405, em = 420/520) and green (ex = 473, em = 490-540) filters. Bars represent means + SEM and different letters within outputs are significantly different (^{ab} $P < 0.05$).

Supplementary Figure S2: Grey-level co-occurrence matrices (GLCM) as a measure of texture of positive staining. A-C) monochlorobimane (MCB, reduced glutathione, GSH); D-F) mitotracker red (active mitochondria) and G-I) peroxyfluor 1 (PF1, H_2O_2). GLCM outputs include angular secondary moment (ASN), contrast and correlation. Data points represent individual oocytes and bars represent mean ± SEM. Different superscripts indicate significant differences (^{ab} $P < 0.05$).

Supplementary Figure S3: Validation of monochlorobimane (MCB) detection of reduced glutathione (GSH) within oocytes by culturing COCs in increasing doses of buthioninesulphoximine (BSO), an inhibitor of glutathione synthesis. Bars represent means + SEM and different letters within outputs are significantly different ($^{ab, x}$ $P < 0.001$).

Table 1. Total amino acid, essential (EA) and non-essential (NEA) amino acid turn over by COCs following cultured in the presence or absence of FSH and BMP15.

Values represent means ± SEM. Negative values represent consumption and positive values represent production.

Table 2. Gene and primer data**.**

SUPPLEMENTARY DATA

Macro 1 (Image processing)

```
open();
run("8-bit");
run("Fit Circle");
// draw circle around embryo and need to insert a command window
makeOval;
setBackgroundColor(255, 255, 255);
run("Clear Outside");
saveAs("Tiff");
```

Macro 2 (Batch Intensity Measure)

```
macro "Batch Measure" {
    dir = getDirectory("Choose a Directory ");
    list = getFileList(dir);
    if (getVersion>="1.40e")
        setOption("display labels", true);
    setBatchMode(true);
    for (i=0; i<list.length; i++) {
        path = dir+list[i];
        showProgress(i, list.length);
        if (!endsWith(path,"/")) open(path);
```

```
847         if (nImages>=1) {
848             run("Measure");
849             close();
850         }
851     }
852 }
853
```

Macro 3 (Batch GLCM Measurements)

```
854 macro "Batch GLCM Measure" {
855     dir = getDirectory("Choose a Directory ");
856     list = getFileList(dir);
857     step = getNumber("Enter the size of the step in pixels: ", 1);
858     setBatchMode(true);
859     print("#,","Angular Second Moment,","Contrast,","Correlation,","Inverse Difference
860 Moment,","Entropy,");
861     for (i=0; i<list.length; i++) {
862         path = dir+list[i];
863         showProgress(i, list.length);
864         if (!endsWith(path,"/")) open(path);
865         if (nImages>=1) {
866             run("GLCM Texture", "enter="+step+ " select=[0 degrees] angular contrast correlation
867 inverse entropy");
868             close();
869             asm = getResult("Angular Second Moment",0);
870             contrast = getResult("Contrast",0);
871
```

```
872             correlation = getResult("Correlation",0);
873             idm = getResult("Inverse Difference Moment   ",0); //Extra spaces needed due to
874     source code error
875             entropy = getResult("Entropy",0);
876             print(list[i],",",asm,",",contrast,",",correlation,",",idm,",",entropy);
877         }
878     }
879 }
```

Figure 1

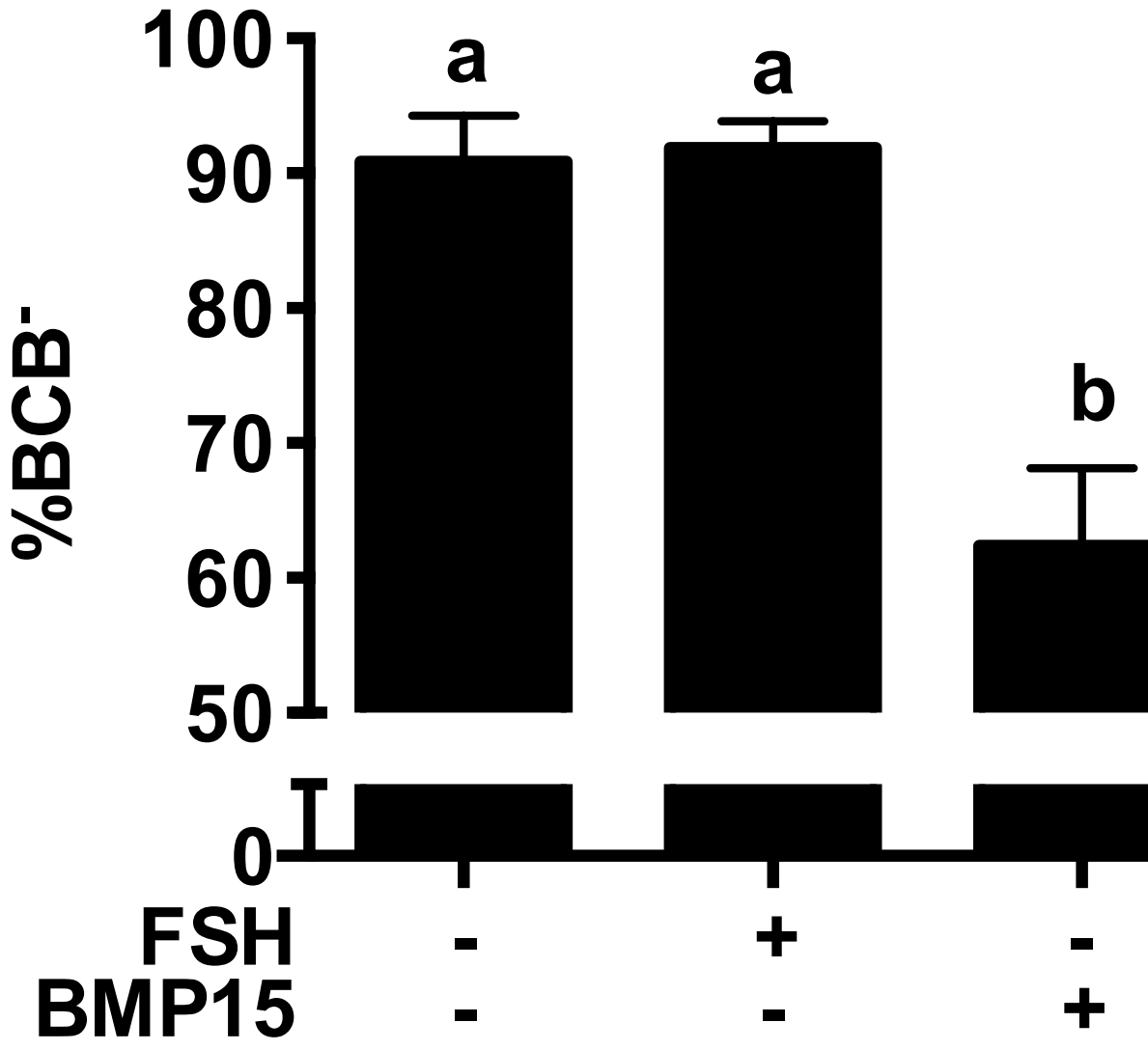

Figure 2

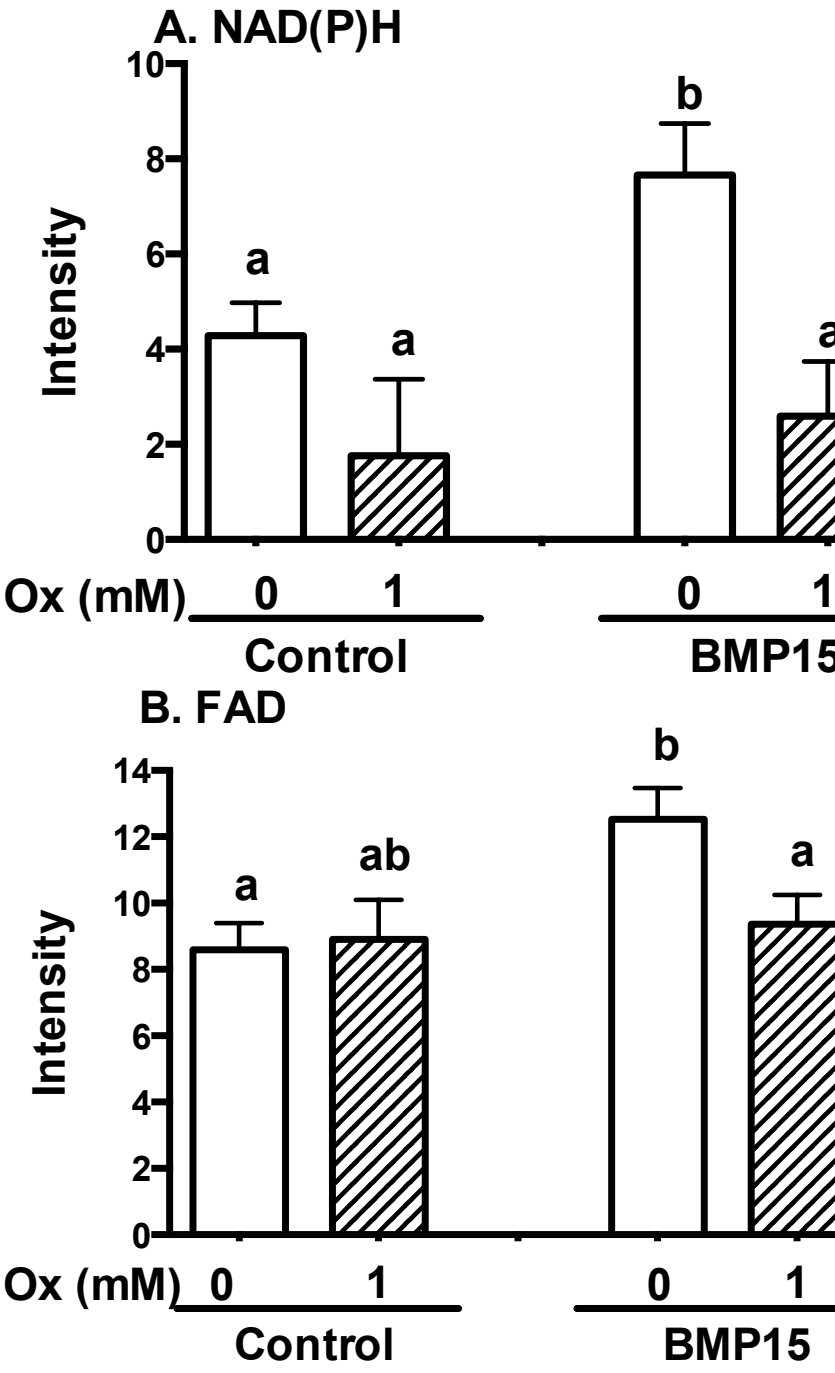
A. NAD(P)H
Intensity
10
8
6
4
2
0
a
a
b
a
Ox (mM) 0 1 0 1
Control
BMP15
B. FAD
Intensity
14
12
10
8
6
4
2
0
a
ab
b
a
Ox (mM) 0 1 0 1
Control
BMP15

Figure 3

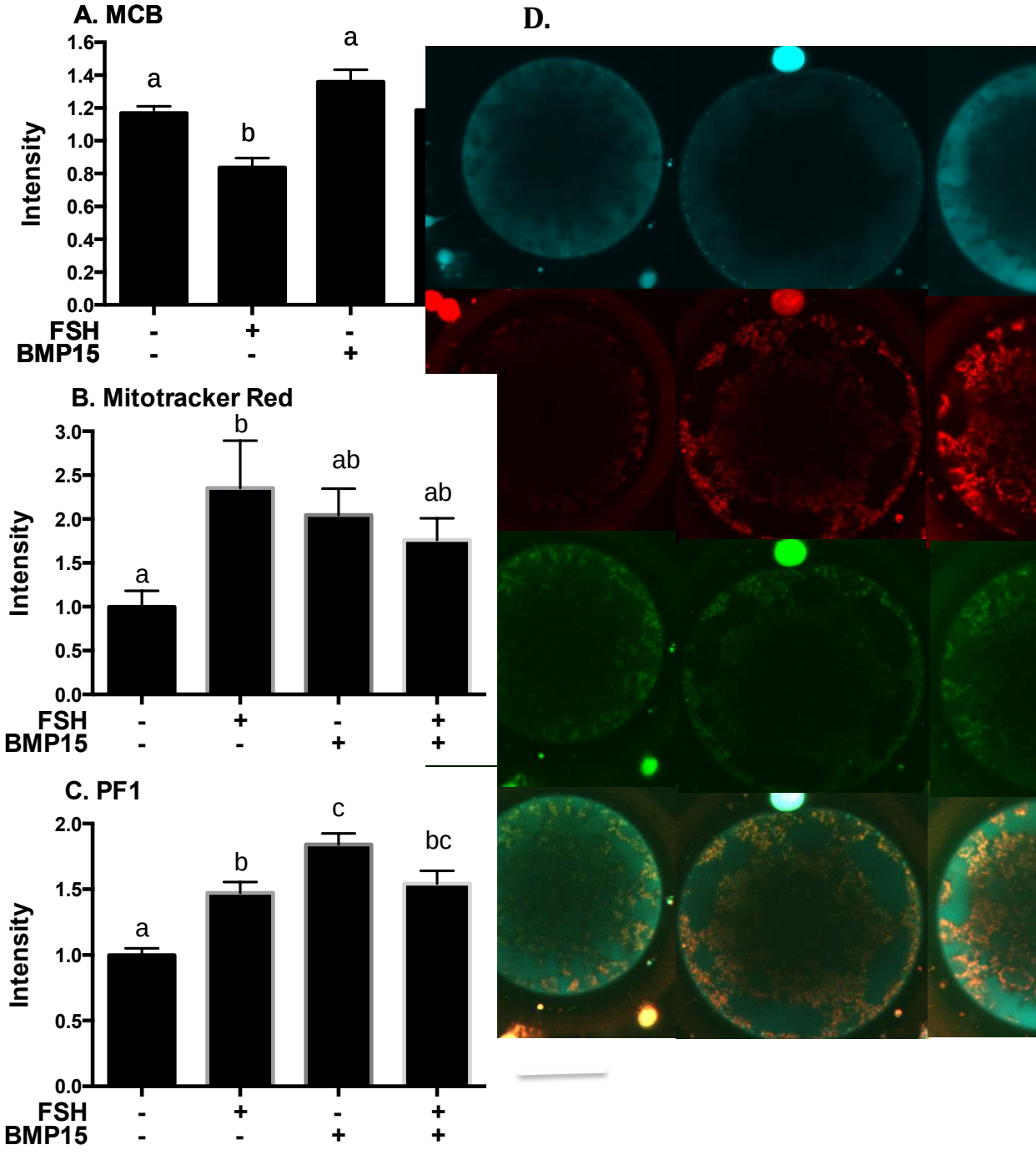
A. MCB
Intensity
1.6
1.4
1.2
1.0
0.8
0.6
0.4
0.2
0.0
a
b
a
FSH - + -
BMP15 - - +
B. Mitotracker Red
Intensity
3.0
2.5
2.0
1.5
1.0
0.5
0.0
a
b
ab
ab
FSH - + - +
BMP15 - - + +
C. PF1
Intensity
2.0
1.5
1.0
0.5
0.0
a
b
c
bc
FSH - + - +
BMP15 - - + +
D.

Figure 4

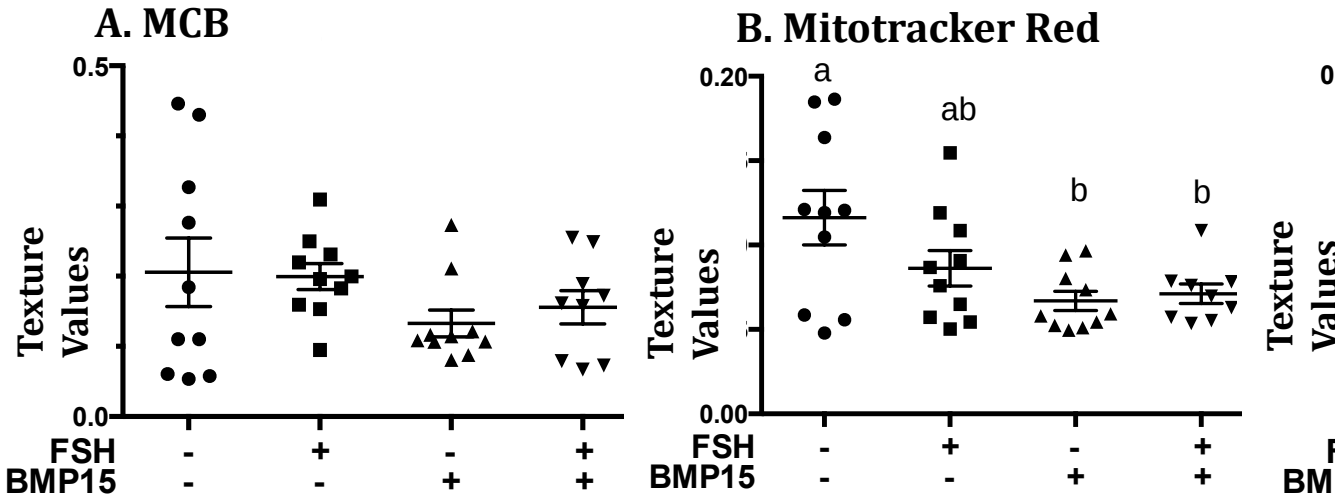
A. MCB
Texture Values
0.5
0.0
FSH - + - +
BMP15 - - + +
B. Mitotracker Red
Texture Values
0.20
0.00
a
ab
b
b
FSH - + - +
BMP15 - - + +

Figure 5

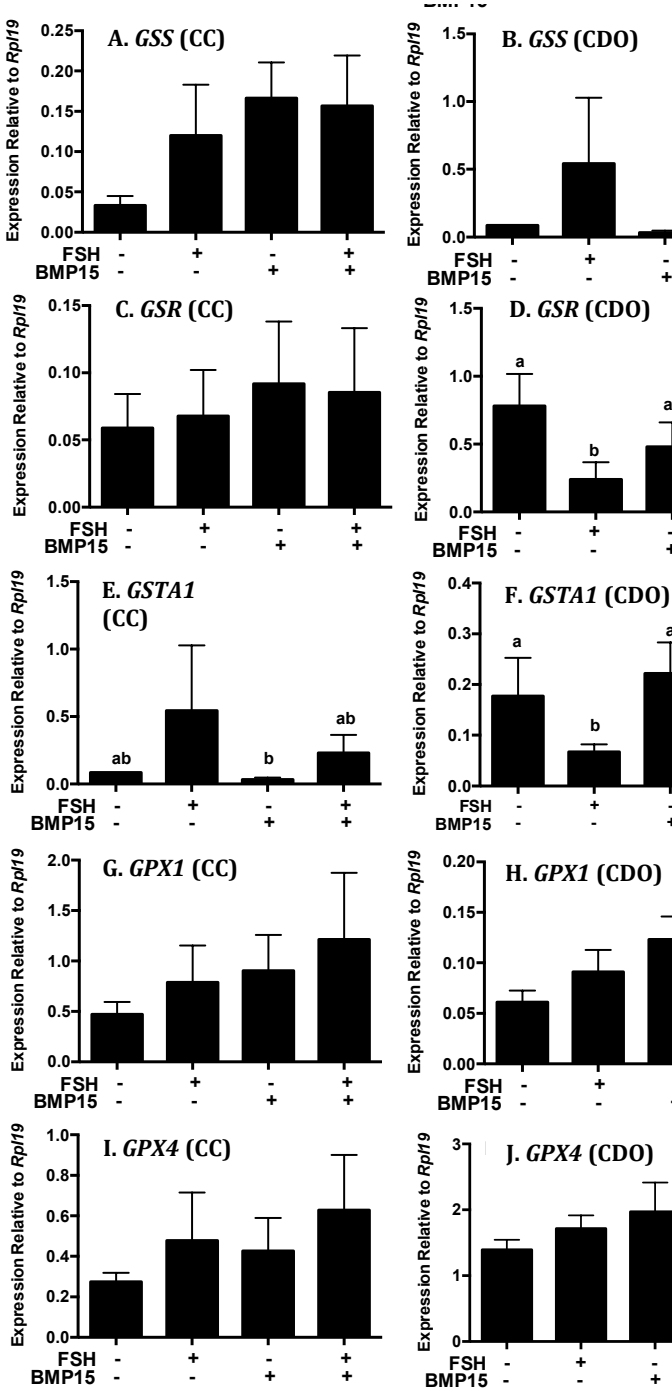
A. GSS (CC)
B. GSS (CDO)
C. GSR (CC)
D. GSR (CDO)
E. GSTA1 (CC)
F. GSTA1 (CDO)
G. GPX1 (CC)
H. GPX1 (CDO)
I. GPX4 (CC)
J. GPX4 (CDO)
Expression Relative to Rpl19
FSH
BMP15
a
b
ab

Figure 6

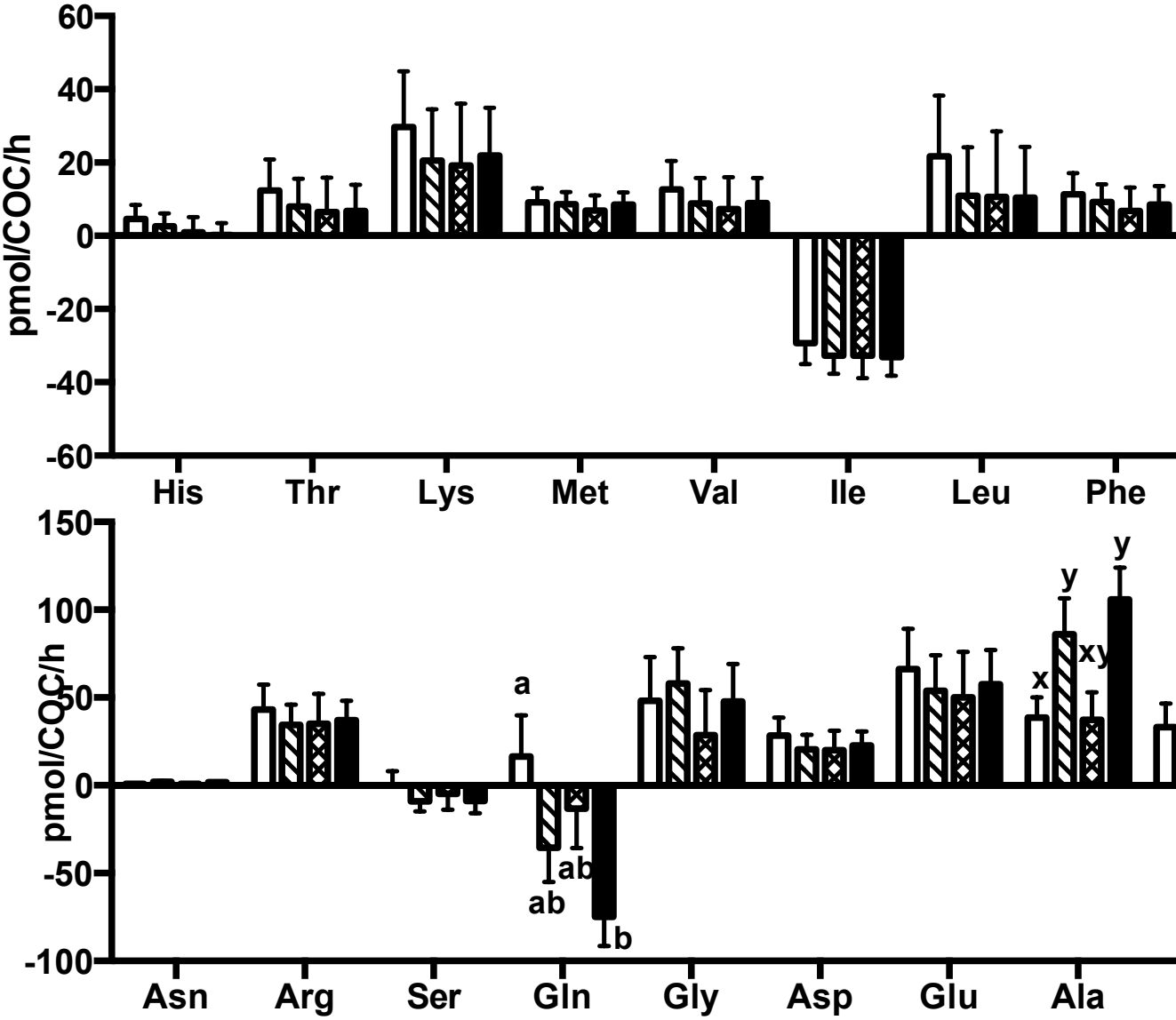
60
40
20
0
-20
-40
-60
pmol/COC/h
His
Thr
Lys
Met
Val
Ile
Leu
Phe
150
100
50
0
-50
-100
pmol/COC/h
a
ab
ab
b
x
y
xy
y
Asn
Arg
Ser
Gln
Gly
Asp
Glu
Ala

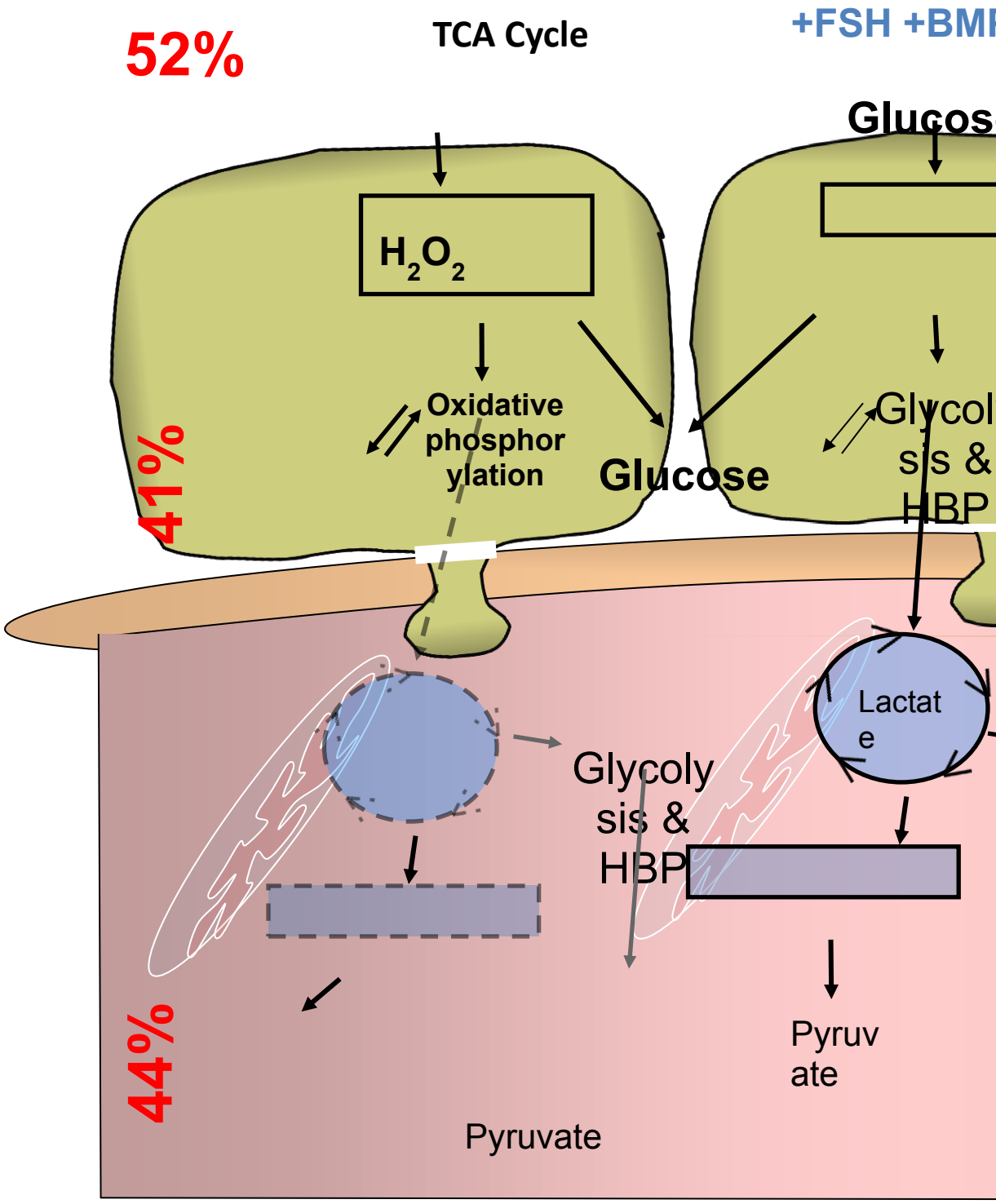
52%
TCA Cycle
+FSH +BMP
Glucos
H_2O_2
Oxidative phosphor ylation
41%
Glucose
Glycol sis & HBP
Lactat e
Glycoly sis & HBP
Pyruv ate
44%
Pyruvate

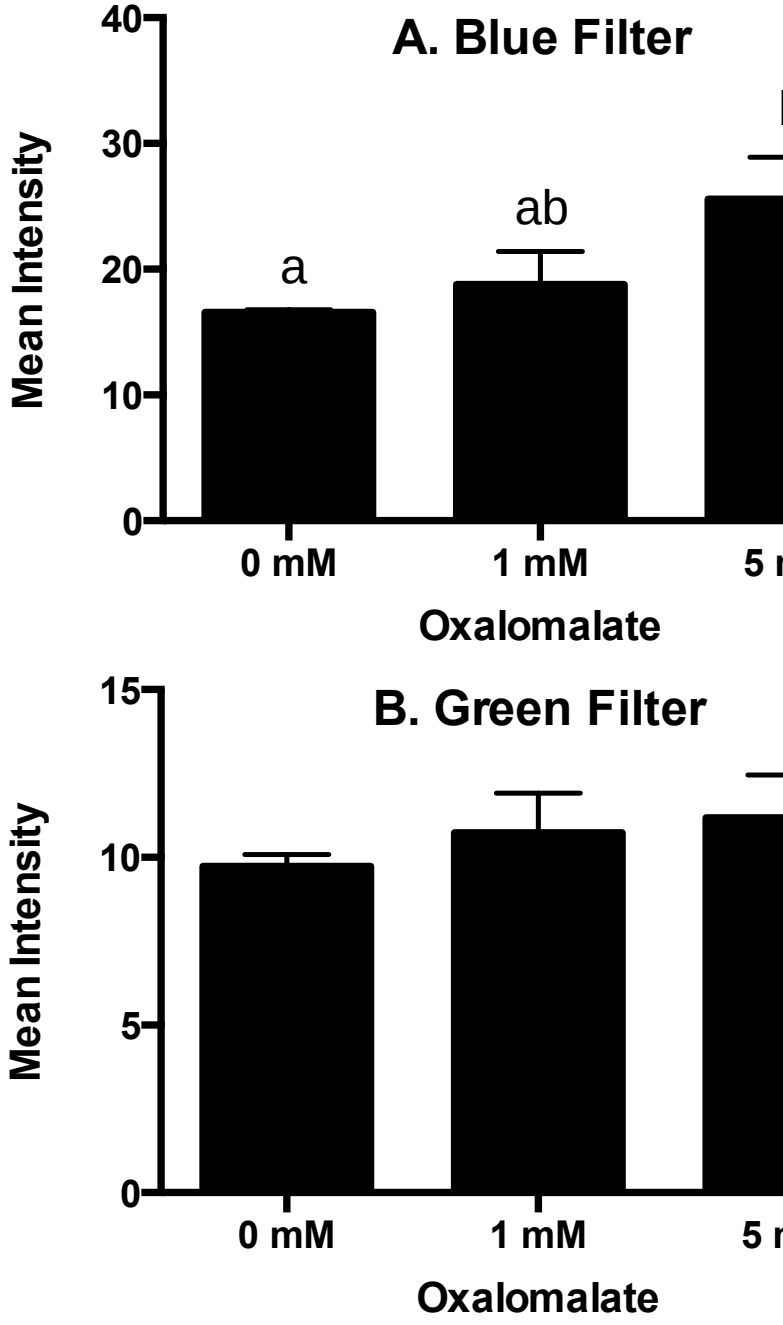
A. Blue Filter
Mean Intensity
40
30
20
10
0
a
ab
0 mM
1 mM
Oxalomalate
B. Green Filter
Mean Intensity
15
10
5
0
0 mM
1 mM
Oxalomalate

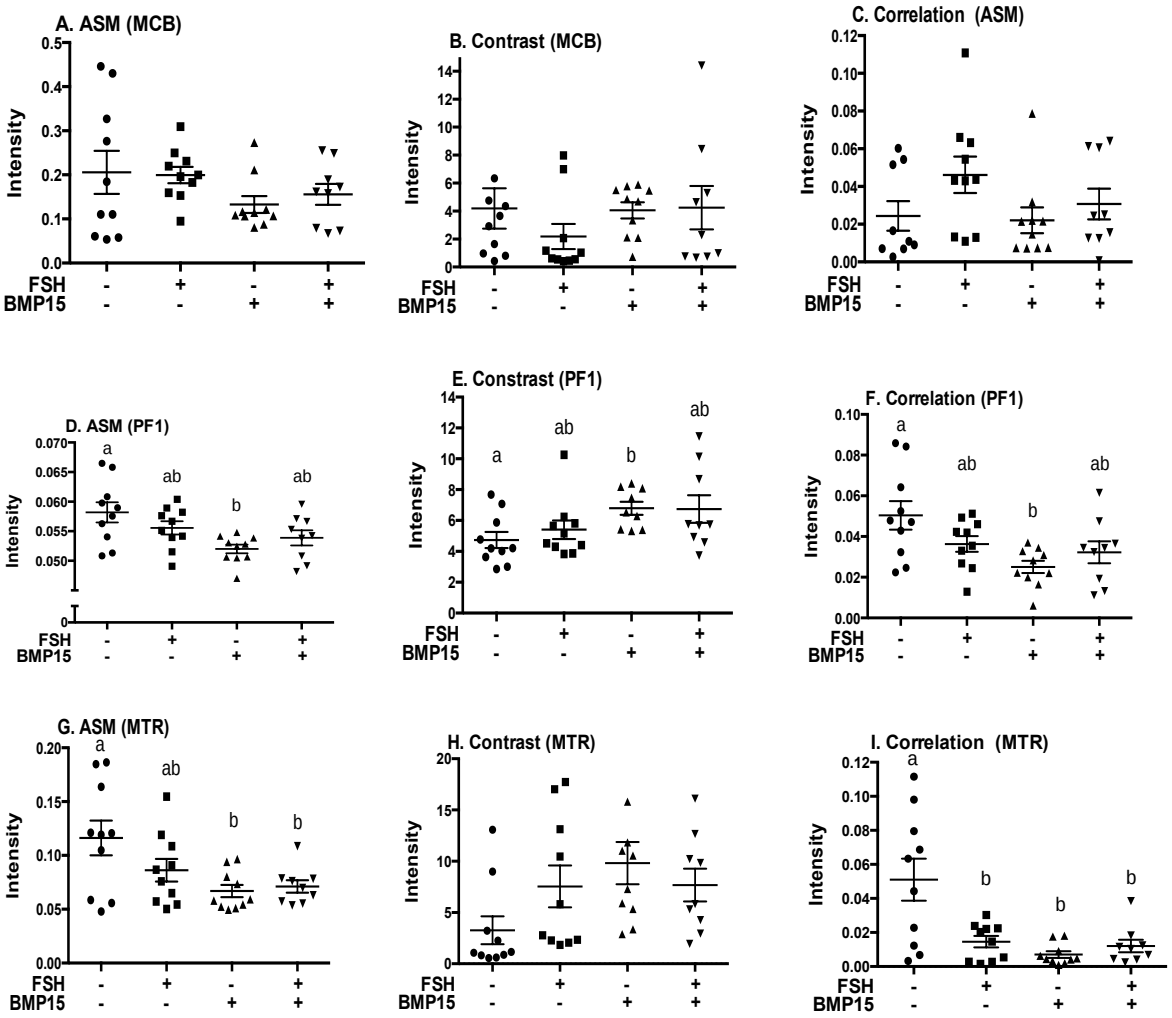
A. ASM (MCB)
B. Contrast (MCB)
C. Correlation (ASM)
D. ASM (PF1)
E. Constrast (PF1)
F. Correlation (PF1)
G. ASM (MTR)
H. Contrast (MTR)
I. Correlation (MTR)
Intensity
FSH
BMP15
a
ab
b

Figure S2

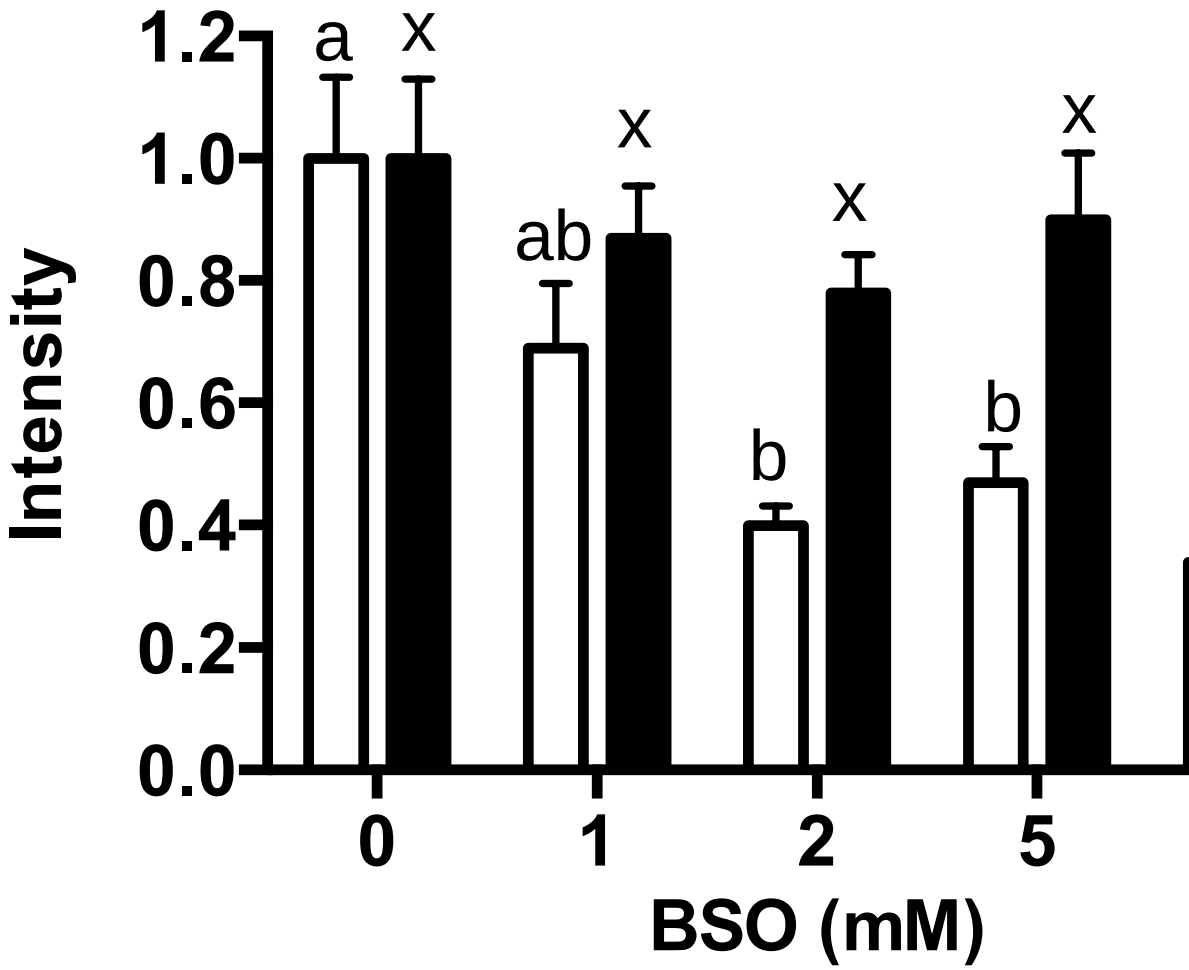
1.2
1.0
0.8
0.6
0.4
0.2
0.0
Intensity
a
x
ab
x
b
x
b
x
0
1
2
5
BSO (mM)